

Experimental investigation of exciton-LO-phonon couplings in CdSe/ZnS core/shell nanorods

Holger Lange,^{1,*} Mikhail Artemyev,² Ulrike Woggon,³ Tore Niermann,⁴ and Christian Thomsen¹

¹*Institut für Festkörperphysik, Technische Universität Berlin, Hardenbergstr. 36, 10623 Berlin, Germany*

²*Institute for Physico-Chemical Problems, Belarusian State University, 14 Leningradskaya Str., Minsk 220080, Belarus*

³*Fachbereich Physik, Universität Dortmund, Otto-Hahn-Str. 4, 44227 Dortmund, Germany*

⁴*Institut für Optik und Atomare Physik, Technische Universität Berlin, Straße des 17. Juni 135, 10623 Berlin, Germany*

(Received 8 February 2008; revised manuscript received 9 April 2008; published 6 May 2008)

We investigate the size dependence of the exciton-LO-phonon coupling strength in colloidal CdSe nanorods coated with an epitaxial ZnS shell. We find an increase in the coupling strength with decreasing nanorod diameter. The growth of a ZnS shell on the nanorod surface much more strongly reduces the exciton-phonon coupling strength than expected from geometry considerations. The determined radius dependence of the Huang-Rhys factor is similar to that observed for spherical CdSe nanocrystals.

DOI: [10.1103/PhysRevB.77.193303](https://doi.org/10.1103/PhysRevB.77.193303)

PACS number(s): 78.30.-j, 78.55.Et, 79.60.Jv, 71.35.-y

I. INTRODUCTION

The coupling between vibrational and electronic excitations has a significant influence on the optical and electrical properties of semiconductors as it determines, e.g., the transport properties and energy relaxation rate of excited carriers. Therefore, the coupling strength is of great importance for semiconductor nanostructures when it comes to applications in the field of optoelectronics. CdSe nanorods have interesting properties, which lead to possible applications in this area, such as low-threshold lasers and photovoltaic devices.^{1,2} The synthesis of colloidal CdSe nanocrystals allows the growth of nanorods with defined radii and lengths.³ The epitaxial growth of a CdS/ZnS graded shell on the CdSe nanorods enhances their optical properties by increasing the luminescence efficiency and decreasing the laser threshold and gives rise to further surface modifications.^{4,5} In the work presented here, we analyze low-temperature Raman spectra to determine the size dependence of the exciton-phonon coupling in CdSe nanorods and the influence of a surrounding ZnS shell on the coupling.

II. EXPERIMENTAL DETAILS

CdSe nanorods of various sizes were grown by a standard technique based on the high temperature (300 °C) reaction between organometallic precursors of Cd (dimethylcadmium) and Se (trioctylphosphine selenide) in trioctylphosphine oxide in the presence of hexadecylphosphonic acid as a surface growth modifier.³ An epitaxial ZnS shell, ~2–3 monolayers in thickness, was grown atop a fraction of selected nanorod samples in a second step in a hexadecylamine/trioctylphosphine oxide reaction mixture at 180 °C, with diethylzinc and thiourea as Zn and S precursors, respectively.⁴ For the Raman measurements, the nanorod samples were deposited on a Si wafer. All of the Raman measurements were performed in a commercial Oxford cryostat at liquid helium temperatures. The 514 nm line of an Ar⁺ laser was used as the excitation source; the laser power was kept below 10 mW to avoid laser heating. A Dilor-XY triple monochromator system in backscattering geometry was used with a nitrogen-cooled charge coupled device to acquire the Raman

spectra. Concomitant to our Raman measurements, we performed high resolution transmission electron microscope (HRTEM) measurements of the CdSe nanorods. The HRTEM micrographs were taken by a Philips CM200-FEG-UT operated at 200 kV.

III. EXPERIMENTAL RESULTS AND DISCUSSION

In polar materials such as CdSe, the dominant coupling between electronic charge and phonons is the Fröhlich interaction between the field induced by the vibrational motion and the electronic charge density. Huang and Rhys⁶ treated the problem with an unperturbed Hamiltonian, neglecting anharmonic coupling between phonons, and an interaction Hamiltonian, which is linear in the vibrational amplitude. The Hamiltonian for each eigenmode of the wave vector \mathbf{k} can then be diagonalized and the problem is equivalent to a shift of the harmonic oscillator potential by an amount Δ_k .⁷ The total coupling can then be characterized by $\Delta^2 = \sum_k \Delta_k^2$, which is equal to the Huang-Rhys factor S .

The Fröhlich interaction between the longitudinal optical (LO) phonons and an exciton can be approximated by the interaction of the LO phonons with a static charge distribution. Following Merlin *et al.*,⁸ the Raman scattering cross section is determined by Franck-Condon overlap integrals, which are algebraic expressions involving Δ . The Raman scattering cross section for an order- n phonon process at low temperatures can be written in the following form:

$$|R^n(\omega)|^2 = \mu^4 \left| \sum_{m=0}^{\infty} \frac{\langle n|m\rangle\langle m|0\rangle}{E_{ij} + n\hbar\omega_{\text{LO}} - \hbar\omega + i\hbar\Gamma} \right|^2, \quad (1)$$

where $\hbar\omega$ is the incident photon energy; E_{ij} is the excited state energy, which is size dependent in the case of confined excitons; μ is the electronic transition dipole moment; Γ is the homogeneous linewidth; and m is an intermediate vibrational level in the excited state.⁹ The vibrational states are considered harmonic oscillator wave functions; the overlap between the ground state and the excited state is given by

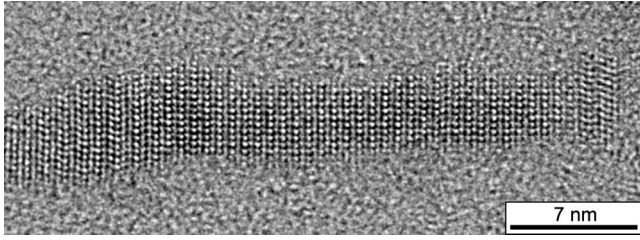


FIG. 1. HRTEM micrograph of a CdSe nanorod coated with a ZnS shell. The amorphous background stems from the supporting carbon grid. Note that it is not possible to differentiate between the core and the shell in the micrograph. The differences in contrast to a few monolayer shells are too small to be resolved due to the microscope's lens aberrations and noise.

$$\langle n|m \rangle = \left(\frac{n!}{m!} \right)^{1/2} \exp\left(-\frac{1}{2}\Delta^2\right) \Delta^{n-m} L_m^{n-m}(\Delta^2), \quad (2)$$

with the Laguerre polynomial L . The value of Δ for a given system can be calculated from the ratio of the integrated intensities of different LO overtones in the Raman spectrum.

Figure 1 displays an exemplary HRTEM micrograph of a CdSe nanorod with a 2–3 monolayer ZnS shell. The nanorods grow along the wurtzite c axis and have weak fluctuations of the diameter along the nanorod. We prepared plain samples of various sizes and investigated the geometry dependence of the exciton-phonon coupling. Figure 2 displays exemplary Raman spectra from the plain CdSe nanorods of 4 nm diameter and 25 nm length at $T=6$ K. Two Raman bands can be identified around 210 and 420 cm^{-1} . The peaks have an asymmetric shape, which we previously explained by the contribution of the LO phonon and surface optical phonons.¹⁰ The underlying CdSe-LO fundamental and its first overtone can be fitted well with Lorentzian functions centered at 209.9 and 421.0 cm^{-1} .

Figure 3 displays the ratio between the integrated intensities of the two- and one LO-phonon Raman bands as a func-

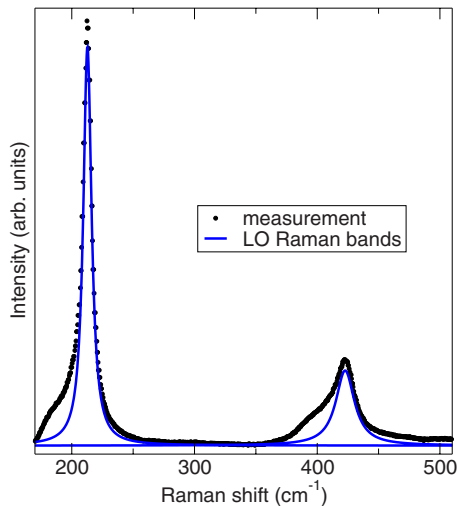


FIG. 2. (Color online) Raman spectra of CdSe nanorods of 4 nm diameter and 25 nm length with underlying Lorentzian-shaped longitudinal optical phonon bands.

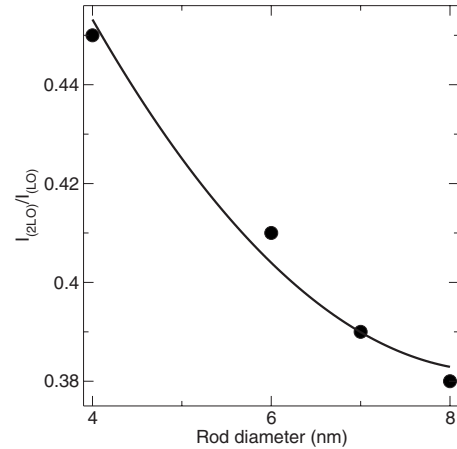


FIG. 3. Diameter dependent ratio of the integrated intensities of the LO fundamental and the first overtone. The solid line is a guide to the eye.

tion of the nanorod diameter. We observe an increase in the ratio of overtone to fundamental with decreasing diameter. Distinct dependences on the nanorod's length or the aspect ratio were not observed. The diameter dependent behavior is very similar to the results for CdSe nanocrystals of 2–3 nm diameter, which was reported by Scamario *et al.*¹¹ The coupling strength scales with the measured ratio and thus increases with decreasing diameter. Nomura *et al.*¹² investigated the spherical CdSe microcrystallites and explained this increase in coupling strength with decreasing size by an increase in the couplings to higher frequency phonons with the reduction of the radius.

The observed similarity between the Huang-Rhys factor of CdSe nanorods and spherical crystals can be assigned to the fluctuations in the confinement potential along the nanorod axis. The nanorod excitons become weakly localized in these thickness fluctuations and experience a rather anisotropic than ideal one-dimensional confinement. The nanorod diameter is thus still the most important geometrical parameter for the exciton confinement. HRTEM measurements performed on a statistical ensemble of nanorods indicate significant fluctuations of the nanorod diameter between the extreme values from 4–7 nm around the mean diameter of 6 nm along the nanorod. This supports our assumption that the excitons do not extend over the whole nanorod length but are confined between diameter constrictions, i.e., they are effectively of the same dimensions as excitons in spherical structures. This coincides with the observations from photoluminescence (PL) measurements. The confinement effects that are observed in the excitonic fine structure also mainly depend on the diameter while being mostly independent of the nanorod length.¹³

Inserting Eq. (2) into Eq. (1) and determining the quotient from $n=2$ and $n=1$ yield an expression that depends on a set of known parameters and the shift Δ only. The Huang-Rhys factor can then be numerically evaluated from the measured ratio by solving the resulting equation for sufficiently large values of m . We have used the measured LO phonon frequency and 514.5 nm photons as exciting photons. For the excitonic transition, we used the results from the spectral

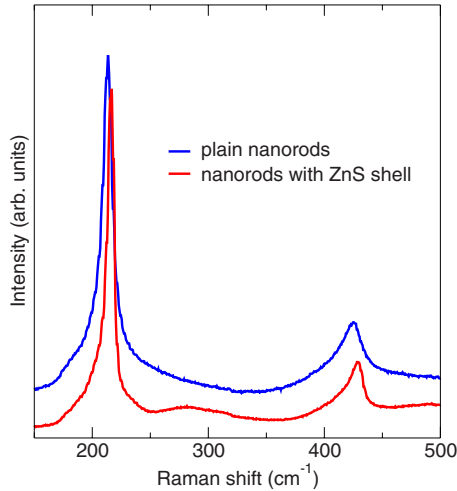


FIG. 4. (Color online) Raman spectra of CdSe nanorods of 8 nm diameter and 80 nm length, which are plain and capped with a 2–3 monolayer ZnS shell.

hole burning measurements on the CdSe nanorods:¹⁴ $\lambda_{\text{ex}} = 590$ nm for the exciton resonance. Numerical evaluations for different energy values due to changing confinement strength for different diameters did not result in significant deviations of S . Thus, we used the noted value for all of the geometries and $\Gamma = 20$ μeV as the approximated linewidth from its determined upper limit of $\Gamma = 10\text{--}20$ μeV . Note that variations in the linewidth do not also have a strong impact on the Huang–Rhys factor. Krauss *et al.*¹⁵ performed a systematic analysis of the influence of the value for the linewidth when calculating the Huang–Rhys factor from the LO overtone to fundamental ratio and demonstrated that the resulting error in S is small. Using the mentioned parameters and the measured ratio of overtone to fundamental results in a Huang–Rhys factor ranging from $S = 0.044$ for our largest structures, which were nanorods of 8 nm diameter, to $S = 0.053$ for the smallest nanorods with a 4 nm diameter. These values are on the order of magnitude of the S values reported for CdSe nanocrystals¹² and comparable to values of the OPL/1LO ratio observed in single nanorod photoluminescence measurements.¹⁶ Nomura *et al.*¹² explicitly calculated the Huang–Rhys factor for a Wannier exciton in bulk CdSe. The obtained value of S strongly depends on the choice of the effective masses for the electron and hole. The

reported values range from $S = 0.38$ to $S = 1.4$.¹² These values are much larger than the Huang–Rhys factor from the nanorods. This is a common experimental observation⁹ that can be explained by the model established by Nomura *et al.*¹² A decreasing importance of the Coulomb interaction and an increasing of confinement effects with decreasing diameter lead to a decreasing Huang–Rhys factor until, at a certain radius, couplings to higher frequency phonons become important and the factor rises again for very small radii.¹²

To investigate the effect of ZnS as boundary, we had two geometries paired as plain CdSe nanorods and CdSe/ZnS core/shell nanorods. Figure 4 displays the Raman spectra from CdSe nanorods of 8 nm diameter and 80 nm length, which are plain nanorods and the same geometry capped with a ZnS shell. The second sample pair was of 4 nm diameter and 25 nm length. The position of the LO phonon from the coated nanorods is shifted due to the strain induced in the CdSe lattice and additional peaks stemming from the shell appear.¹⁰ Table I summarizes the relevant data for all LO-phonon Raman bands. The trends of the changes are similar for both geometries.

The ratio of LO overtone to the fundamental is significantly reduced for the coated nanorods. The Huang–Rhys factor is reduced by 18% for the larger CdSe nanorods and by 43% for the smaller CdSe nanorods when adding a ZnS shell. These changes are much larger than one would expect from the diameter dependence. By extrapolating the trend of the diameter dependent measurements, the increase in the diameter due to the additional shell would lead to changes less than 2%. It is important to notice that the shell has a much greater impact on the small geometry than on the larger nanorods. The difference in S observed between nanorods with and without a ZnS shell can be attributed to the changed confining potential for the electron and hole wave function. A different increase in the confining potential for electrons and holes, as a result of the ZnS shell growth, results in a reduced polarity of the exciton wave function and thus a reduction of the coupling. Another reason for the decreased coupling, which strengthens the effect of the confinement, is the reduced Fröhlich coupling in mixed fractions of Cd and Zn. Small amounts of CdZn compounds are expected to be present in the surface regions after the epitaxial growth of the shell. Zheng *et al.*¹⁷ did a theoretical investigation of exciton-LO-phonon interactions in zinc compounds. They applied a mixed crystal theory on zinc com-

TABLE I. CdSe longitudinal optical phonons. The spectra were normalized to the LO fundamental.

	Sample type			
	4×25 nm ² core	4×25 nm ² core/shell	8×80 nm ² core	8×80 nm ² core/shell
LO position (cm ⁻¹)	209.9	210.8	213.3	216.1
2LO position (cm ⁻¹)	421.0	423.9	425.4	428.3
LO area (arb. units)	11.76	10.22	11.76	8.53
2LO area (arb. units)	5.35	2.58	4.51	2.81
$I_{2\text{LO}}/I_{\text{LO}}$	0.45	0.25	0.38	0.33
S	0.053	0.030	0.044	0.036

pounds to calculate the exciton-LO-phonon interaction energies and discovered a reduced electron-LO-phonon interaction in mixed $Zn_xCd_{1-x}Se$ compounds with rising Zn content. The sum of both effects, in addition to the decrease in S due to the increased diameter, can explain the strong reduction in the coupling strength. Both effects also explain the large deviation in the change of the Huang-Rhys factor between the small and the large nanorods. The surface-to-volume ratio of the nanorods reciprocally scales with the radius. The amount of mixed CdZn compounds in the surface region comparative to the total nanorod volume is much larger in the small nanorods than in the larger structures. Furthermore, the influence of the changed confining potential on the exciton wave function is larger for the stronger localized excitons in the small nanorods.

IV. CONCLUSIONS

We have investigated exciton-LO-phonon couplings in CdSe nanorods. The Huang-Rhys factor in CdSe nanorods is

much smaller than in bulk CdSe and scales between $S=0.044$ and $S=0.053$ within the investigated diameter regime of 4–8 nm. For CdSe nanorods of those sizes, the Huang-Rhys factor increases with decreasing diameter. This behavior is similar to that of spherical CdSe nanocrystals and can be explained by an increase in coupling to higher frequency phonons for small radii and a confinement of the excitons between diameter fluctuations of the nanorods. When coating the nanorods with an epitaxial ZnS shell, the Huang-Rhys factor is noticeably reduced, which can be explained by the increased confinement of the exciton wave function and is accompanied by a decrease due to the reduced exciton-LO-phonon interaction in CdZn compounds and the presence of mixed CdZnSe compounds at the nanorod's surface after the epitaxial growth of the shell.

ACKNOWLEDGMENTS

We acknowledge Marcel Mohr for helpful suggestions on the numerical analysis and the DFG for financial support with Grant No. SPP 1165.

*holger.lange@physik.tu-berlin.de

¹M. Kazes, D. Lewis, Y. Ebenstein, T. Mokari, and U. Banin, *Adv. Mater. (Weinheim, Ger.)* **14**, 317 (2002).

²W. Huynh, J. Dittmer, and A. Alivisatos, *Science* **295**, 2425 (2002).

³X. Peng, L. Manna, W. Yang, J. Wickham, E. Scher, A. Kadavanich, and A. P. Alivisatos, *Nature (London)* **404**, 59 (2000).

⁴L. Manna, E. Scher, L. Li, and A. Alivisatos, *J. Am. Chem. Soc.* **124**, 7136 (2002).

⁵D. Gerion, F. Pinaud, S. Williams, W. Parak, D. Zanchet, S. Weiss, and A. Alivisatos, *J. Phys. Chem. B* **105**, 8861 (2001).

⁶K. Huang and A. Rhys, *Proc. R. Soc. London, Ser. A* **204**, 406 (1950).

⁷C. Duke and G. Mahan, *Phys. Rev.* **139**, A1965 (1965).

⁸R. Merlin, G. Güntherodt, R. Humphreys, M. Cardona, R. Suryanarayanan, and F. Holtzberg, *Phys. Rev. B* **17**, 4951 (1978).

⁹A. P. Alivisatos, T. D. Harris, P. J. Carroll, M. L. Steigerwald, and L. E. Brus, *J. Chem. Phys.* **90**, 3463 (1989).

¹⁰H. Lange, M. Machón, M. Artemyev, U. Woggon, and C. Thomsen, *Phys. Status Solidi (RRL)* **1**, 274 (2007).

¹¹G. Scamarcio, V. Spagnolo, G. Ventruti, M. Lugará, and G. C. Righini, *Phys. Rev. B* **53**, R10489 (1996).

¹²S. Nomura and T. Kobayashi, *Phys. Rev. B* **45**, 1305 (1992).

¹³N. Le Thomas, E. Herz, O. Schöps, U. Woggon, and M. V. Artemyev, *Phys. Rev. Lett.* **94**, 016803 (2005).

¹⁴S. Tavenner-Kruger, Y. Park, M. Lonergan, U. Woggon, and H. Wang, *Nano Lett.* **6**, 2154 (2006).

¹⁵T. D. Krauss and F. W. Wise, *Phys. Rev. B* **55**, 9860 (1997).

¹⁶T. Potjans, *Diplomarbeit thesis*, Technical University Dortmund, 2005.

¹⁷R. Zheng, M. Matsuura, and T. Taguchi, *Phys. Rev. B* **61**, 9960 (2000).